

Structural Characterization of Novel Ionic Materials Incorporating the Bis(trifluoromethanesulfonyl)amide Anion

C. M. Forsyth,* D. R. MacFarlane, J. J. Golding, J. Huang, J. Sun, and M. Forsyth

School of Chemistry and School of Physics and Materials Engineering,
Monash University, Clayton, Victoria 3800, Australia

Received August 29, 2001. Revised Manuscript Received December 14, 2001

A range of low melting salts of the bis(trifluoromethanesulfonyl)amide (TFSA) anion with hindered organic cations (*N*-methyl-1-methylpyrrolinium, *N,N*-dimethylpyrrolidinium, *N,N,N*-trimethylammonium, and *N,N,N,N*-tetrakis(*n*-propyl)ammonium) have been crystallized. Single-crystal X-ray diffraction data show these materials to consist of discrete ions with only weak C–H…O (or for Me_3NH N–H…O) contacts between the constituent atoms of the cations and anions close to the limits of van der Waals separations. Consequently, the observed physical properties of these materials presumably result from the diffuse negative charge on the TFSA anion and inefficient packing of these large and irregularly shaped ions.

Introduction

Classical inorganic salts consist of infinite three-dimensional arrays of close packed spherical ions and are characteristically brittle solids with high melting points (e.g., mp of NaCl is 801 °C). In contrast, ionic materials possessing hindered organic cations combined with an anion having a diffuse negative charge are often low melting or even liquid at room temperature.^{1,2} Furthermore, in some cases, these fascinating materials exhibit numerous solid–solid phase transitions possibly derived from a progressive onset of dynamic rotational and/or translational motion of one or more ions (plastic crystal phases) from an ordered low-temperature phase.^{1,2} Their desirable physical properties have attracted interest as environmentally friendly reaction media for chemical synthesis,³ and they are also promising electrolyte materials.^{4,5} For example, when doped with 1–5 mol % of lithium ions, these electrolytes exhibit fast ion conduction in the solid state leading to potential applications in lithium batteries.^{4,5} A prominent anion in these new materials is the bis(trifluoromethanesulfonyl)amide ion (TFSA) (I) (Figure 1). Delocalization of the negative charge within the S–N–S backbone of the TFSA anion combined with steric protection provided by the sulfonyl oxygen atoms and the CF₃ groups presumably decreases ion–ion interactions within the solid thus facilitating ion mobility. The TFSA anion has been shown to significantly depress the melting tem-

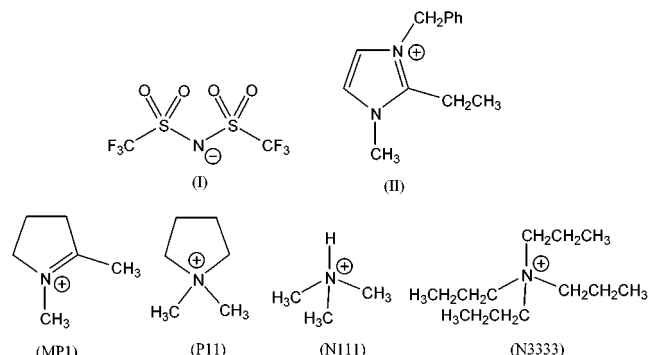


Figure 1.

peratures of tetraalkylammonium or *N,N*-dialkylpyrrolidinium salts by up to 100 °C relative to the corresponding halides.^{6,7}

The elucidation of the structures for these materials would yield important information concerning the spatial relationships of the relative ions and the degree of ion interactions in the solid state. These data may also have further implications, providing a basis for the interpretation of the dynamic disorder in the higher temperature phases of these materials. For example, rotational disorder of the periodate anion in [NMe₄]₂[IO₄]⁸ was characterized in detail from single-crystal X-ray structural data. Such data might also provide insight into the possible role of the Li⁺ cations when these salts are doped with [Li(TFSA)]_{...}. However, X-ray structures of salts of the TFSA anion are relatively scarce. Despite the delocalization of the negative charge

* To whom correspondence should be addressed.

(1) Bonhote, P.; Dias, A. P.; Papageorgiou, N.; Kalanasundaram, K.; Gratzel, M. *Inorg. Chem.* **1996**, *35*, 1168.

(2) MacFarlane, D. R.; Meakin, P.; Amini, N.; Forsyth, M. *J. Phys.: Condens. Matter* **2001**, *13*, 8257.

(3) Welton, T. *Chem. Rev.* **1999**, *99*, 2071.

(4) MacFarlane, D. R.; Huang, J.; Forsyth, M. *Nature* **1999**, *402*, 792.

(5) Forsyth, M.; MacFarlane, D. R.; Huang, J. *J. Mater. Chem.* **2000**, *10*, 2259.

(6) MacFarlane, D. R.; Meakin, P.; Sun, J.; Amini, N.; Forsyth, M. *J. Phys. Chem. B* **1999**, *103*, 4164.

(7) MacFarlane, D. R.; Sun, J.; Golding, J.; Meakin, P.; Forsyth, M. *Electrochim. Acta* **2000**, *45*, 1271.

(8) Wagner, R. I.; Bau, R.; Gnann, R. Z.; Jones, P. F.; Christie, K. O. *Inorg. Chem.* **1997**, *36*, 2564.

Table 1. Crystal and Refinement Data

compound formula	[N111][TFSA] ^a C ₅ H ₁₀ F ₆ N ₂ O ₄ S ₂	[MP1][TFSA] C ₇ H ₁₂ F ₆ N ₂ O ₄ S ₂	[P11][TFSA] C ₈ H ₁₄ F ₆ N ₂ O ₄ S ₂	[N3333][TFSA] ^b C ₁₄ H ₂₁ F ₆ N ₂ O ₄ S ₂
<i>M</i>	340.27	378.82	380.33	466.51
<i>T</i>	133	123	123	173
crystal system	monoclinic	monoclinic	monoclinic	monoclinic
space group	<i>P</i> 2 ₁ / <i>c</i> (No. 14)	<i>P</i> 2 ₁ / <i>n</i> (No. 14)	<i>P</i> 2 ₁ / <i>c</i> (No. 14)	<i>P</i> 2 ₁ / <i>n</i> (No. 14)
<i>a</i> (Å)	7.6084(1)	8.1121(2)	8.5034(2)	9.7417(1)
<i>b</i> (Å)	14.2150(3)	14.5315(5)	13.8305(4)	22.8615(3)
<i>c</i> (Å)	12.5086(2)	12.8176(3)	12.8083(3)	10.0251(1)
β (°)	106.552(1)	103.979(2)	98.785(2)	97.620(1)
<i>V</i> (Å ³)	1296.8(4)	1466.2(5)	1488.7(5)	2213.0(8)
<i>Z</i>	4	4	4	4
ρ_{calcd} (g cm ⁻³)	1.743	1.714	1.697	1.400
μ (Mo K α) (mm ⁻¹)	0.495	0.448	0.441	0.310
crystal size	0.25 × 0.25 × 0.25	0.13 × 0.13 × 0.30	0.13 × 0.20 × 0.25	0.10 × 0.15 × 0.33
<i>F</i> (000)	688	768	776	976
2 <i>θ</i> _{max} (deg)	56.6	56.5	55.7	56.8
<i>N</i> (<i>R</i> _{int})	3188 (0.039)	3628 (0.053)	3510 (0.044)	5483 (0.049)
<i>N</i> _o	2710	2367	2634	3800
<i>R</i> , <i>R</i> _w [<i>I</i> > 2 <i>s</i> (<i>I</i>)]	0.0314, 0.0788	0.054, 0.118	0.037, 0.075	0.046, 0.104
<i>R</i> , <i>R</i> _w (all data)	0.0401, 0.0840	0.101, 0.141	0.062, 0.083	0.080, 0.117
goodness of fit	1.080	1.052	1.027	1.032
$\Delta e_{\text{min,max}}$ (e Å ⁻³)	-0.494, 0.282	-0.463, 0.436	-0.368, 0.279	-0.33, 0.45

^a Cell parameters at 273 K: *a* = 7.7665(1), *b* = 14.3160(3), and *c* = 12.7511(3) Å, β = 106.958(1)°, *V* = 1356.1 Å³. ^b Cell parameters at 295 K: *a* = 9.8384(2), *b* = 23.0065(5), and *c* = 10.1832(2) Å, β = 97.859(3)°, *V* = 2283.3 Å³.

in the TFSA anion, the pure [Li(TFSA)]_∞⁹ and [K(TFSA)]_∞¹⁰ salts have strong cation–anion interactions through coordination of the oxophilic alkali metal cations to the sulfonyl oxygen atoms of several TFSA anions resulting in extended network structures. Even when dissolved in a polyether, some residual Li–TFSA bonding persists as shown by the structure of [(PEO)₃:Li(TFSA)] which has lithium coordination by three ether oxygen atoms but also by two sulfonyl oxygen atoms from separate TFSA anions.¹¹ Alternatively, [Mg(H₂O)₆]²⁺[TFSA]₂·2H₂O¹² and [Yb(L)₆]³⁺[TFSA]₃¹³ (L = *N,N*-dimethylpropyleneurea) have the metal cations completely separated from the anions by the coordinated ligands. However, in the Mg salt, the ions still associate through hydrogen bonding between the water molecules (both coordinated and lattice) and the sulfonyl oxygen atoms.¹² Notably, the sole structure of an organic TFSA salt, with the 1-ethyl-2-methyl-3-benzyl imidazolium cation (II) (Figure 1),¹⁴ shows no such strong inter-ion contacts and this is clearly an important factor governing the desirable physical properties of these ionic materials. Given the importance of the TFSA anion in the solid electrolyte field and the paucity of structural information, we have crystallized and now report the structures of some organic TFSA salts with the following cations: *N*-methyl-1-methylpyrrolinium (MP1), *N,N*-dimethylpyrrolidinium (P11), *N,N,N,N*-trimethylammonium (N111), and *N,N,N,N*-tetrakis(*n*-propyl)ammonium (N3333). The cations chosen for this study present different geometrical requirements, being at the extremes, from almost planar (MP1) to fully tetrahedral (N3333) (Figure 1).

(9) Nowinski, J. L.; Lightfoot, P.; Bruce, P. G. *J. Mater. Chem.* **1994**, 4, 1579.
 (10) Zak, Z.; Ruzicka, A.; Michot, C. *Z. Kristallogr.* **1998**, 213, 217.
 (11) Andreev, Y. G.; Lightfoot, P.; Bruce, P. G. *J. Appl. Crystallogr.* **1997**, 18, 294.
 (12) Hass, A.; Klare, C.; Bruckmann, J.; Kruger, C.; Tsay, Y.-H.; Aubke, F. *Inorg. Chem.* **1996**, 35, 1918.
 (13) Mikami, K.; Kotera, O.; Motoyama, Y.; Tanaka, M. *Inorg. Chem. Commun.* **1998**, 1, 10.
 (14) Golding, J. J.; MacFarlane, D. R.; Spiccia, L. S.; Forsyth, M.; Skelton, B. W.; White, A. H. *Chem. Commun.* **1998**, 1593.

Experimental Section

The preparation and properties of [MP1][TFSA] (mp 113 °C), [P11][TFSA] (mp 132 °C), and [N3333][TFSA] (mp 105 °C) have been described elsewhere.^{6,7,15} The new salt [N111][TFSA] was synthesized by reaction of Me₃NHCl (0.58 g, 6.0 mmol) and Li(TFSA) (1.63 g, 6.0 mmol) in water (50 mL). The colorless salt was crystallized after reducing the volume of the solution and then dried under vacuum, resulting in a yield of 52% (1.07 g): mp 79–81 °C. IR(Nujol): 3180m, 1330s, 1246m, 1207s, 1190s, 1135m, 1056s, 978m, 749w, 743w cm⁻¹. ¹H NMR (200 MHz, CDCl₃): δ 1.61 (br s, 1H, NH), 2.96 (s, 9H, Me). Anal. Calcd for (C₅H₁₀F₆N₂O₄S₂ 340.25): C, 17.65; H, 2.96; N, 8.23. Found: C, 17.78; H, 3.08; N, 8.25.

All four TFSA salts were crystallized from aqueous solutions as colorless needles or plates and were used without drying for single-crystal X-ray diffraction experiments. For each data collection, a representative clear colorless specimen was cut from a larger crystal, covered in viscous oil, and then mounted onto a glass fiber. A sphere of diffraction data was collected on rapidly cooled (for data collection temperatures see Table 1) samples using an Enraf-Nonius CCD area detector diffractometer (Mo K α radiation, λ = 0.71073 Å, crystal to detector distance = 30.0 mm, 1.0° frames in φ and ω , exposure = 10–30 s per frame). In some cases, comparative data were also collected at or near room temperature. The raw images were processed using proprietary software (Nonius BV 1997) yielding sets of unique data after merging which were used for structure solution by direct methods and subsequent full matrix least-squares refinement cycles (SHELX 97). All non-hydrogen atoms were refined with anisotropic thermal parameters. Hydrogen atoms for the P11 and N111 cations were located in the difference Fourier and were allowed to freely refine; all other hydrogen atoms were placed in calculated positions using a riding model. Crystal and refinement data for each salt are listed in Table 1, and selected bond distances and angles are listed in Tables 2–4.

Results and Discussion

For bulk samples of [MP1][TFSA] and [N3333][TFSA] no significant thermal events were detected by DSC between low and room temperatures,^{7,15} whereas [P11][TFSA] exhibits a weak phase transition near –20 °C.⁶

(15) MacFarlane, D. R.; Sun, J.; Forsyth, M. *J. Mater. Chem.*, submitted, 2001.

While the DSC results do not exclude the existence of structurally significant phase change (for example, see ref 8), rapid cooling through such a solid–solid-phase transition would be expected to give a polycrystalline sample resulting in splitting of the diffracted X-rays (e.g., twinning), as was observed during attempts to cool single crystals of $[\text{NMe}_4]\text{[IO}_4]$,⁸ and there was no evidence of this effect in the diffraction patterns of the four TFSA salts. Furthermore, 0 °C and room-temperature data collection and structure solutions for $[\text{N}111]\text{[TFSA]}$ and $[\text{N}3333]\text{[TFSA]}$, respectively, were consistent with the low-temperature determinations (see below).

The $[\text{MP1}]\text{[TFSA]}$, $[\text{P}11]\text{[TFSA]}$, $[\text{N}111]\text{[TFSA]}$, and $[\text{N}3333]\text{[TFSA]}$ salts crystallize in monoclinic lattices (Table 1) similar to that of $[\text{II}]\text{[TFSA]}$.¹⁴ Each has four pairs of ions occupying the unit cell, the asymmetric component comprising one discrete ion pair (Figures 2–5). The structures of $[\text{P}11]\text{[TFSA]}$ and $[\text{N}111]\text{[TFSA]}$ are fully ordered; however, the data for $[\text{MP1}]\text{[TFSA]}$ and $[\text{N}3333]\text{[TFSA]}$ indicated the presence of disorder in the cations. For the MP1 cation, the pyrrolinium ring was refined in two positions (refined occupancies 0.652(7):0.348(7)) rotated within the ring plane by approximately 180° with C(1), C(3), and C(6) common to both disordered components (Figure 2a). Similarly, each of the propyl groups of the N3333 cation takes up two orientations (refined occupancies 0.718(3):0.282(3)) each with a shared γ-carbon (Figure 5a). The MP1 cation has not been previously structurally characterized; however, orientational disorder in the N3333 cation was reported in the room-temperature structure of $[\text{N}3333]\text{[BF}_4]$.¹⁶ The observed cation disorder in the TFSA salts does not appear to indicate solid-state molecular motion and is unlike the near continuous rotation of tetrahedral anions characterized in the structures of $[\text{NMe}_4]\text{[IO}_4]$ ⁸ and $[\text{NMe}_4]\text{[BF}_4]$ ¹⁷ in nonordered higher temperature phases. For $[\text{N}3333]\text{[BF}_4]$, two solid–solid transitions at 289 and 392 K have been detected by DSC.¹⁸ NMR data for this material have suggested that reorientation of the methyl groups occurs with additional reorientations of the alkyl chains with increasing temperature ultimately leading to overall cation motion at the higher temperature transition.¹⁹ This type of cation motion is different from the current structural model which shows disorder in the methylene sites only.

The bond distances and angles of the nonplanar P11 (Figure 3), N111 (Figure 4), and the disordered N3333 (Figure 5) cations are very similar to those in $[\text{P}11]\text{[I]}$,²⁰ $[\text{N}111]\text{[BPh}_4]$,²¹ and $[\text{N}3333]\text{[BF}_4]$,¹⁶ respectively. In contrast, the non-hydrogen atoms of the previously uncharacterized MP1 cation (Figure 2) are almost planar (maximum deviation from the mean plane = 0.08 Å), presumably due to the constraints imposed by the

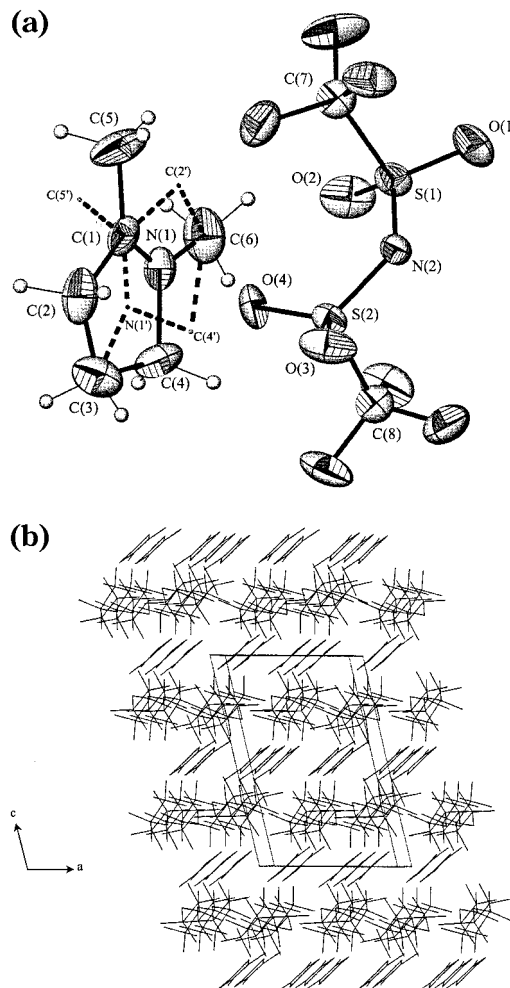


Figure 2. (a) Molecular structure of $[\text{MP1}]\text{[TFSA]}$ showing one ion pair. The position of the second component of the disordered MP1 cation is indicated by the dotted lines. (b) The extended structure of $[\text{MP1}]\text{[TFSA]}$ showing the layers of cations and anions parallel to the 010 plane (hydrogen atoms and the second component of the disordered MP1 cation have been omitted for clarity).

N=C double bond within the five-membered ring. Consistent with the presence of the double bond, the N(2)–C(1) distance is 0.27 Å shorter than the corresponding N(2)–C(4) distance (Table 2).

The bond distances and angles of the TFSA anions in all four salts are similar (Table 3) and virtually indistinguishable from those observed in $[\text{II}]\text{[TFSA]}$,¹⁴ consistent with dispersion of the negative charge across the S–N–S framework. The S–CF₃ groups are orientated exclusively trans (torsion angles C–S–S–C (°) MP1, 174.6(2); P11, 173.4(1); N111, 173.85(8); N3333, 166.3(1)). This is the lower energy configuration,¹⁰ and a cis orientation is generally observed only in the presence of an external interaction with the sulfonyl oxygen atoms (e.g., chelation to K⁺ in $[\text{K}(\text{TFSA})]_\infty$).¹⁰ The TFSA anion can be compared to its nonfluorinated analogue, for example, in $[\text{Me}_2\text{NH}_2]\text{[N}(\text{SO}_2\text{CH}_3)_2]$.²² The N(SO₂CH₃)₂ anion is also in a trans configuration but the torsion angle is considerably reduced (C–S–S–C = 130.7 °). Small increases (0.01–0.02 Å) in the N–S and S–O distances are also observed, but the S–C

(16) Giuseppetti, G.; Mazzi, F.; Tadini, C.; Ferloni, P.; Zabinska, G.; Torre, S. *Z. Kristallogr.* **1997**, *211*, 367.

(17) Giuseppetti, G.; Mazzi, F.; Tadini, C.; Ferloni, P.; Torre, S. *Z. Kristallogr.* **1992**, *202*, 81.

(18) Zabinska, G.; Ferloni, P.; Sanesi, M. *Thermochim. Acta* **1987**, *122*, 87.

(19) Szafranska, B.; Pajak, Z. *Z. Naturforsch., A* **1995**, *50*, 584.

(20) Golding, J.; Hamid, N.; MacFarlane, D. R.; Forsyth, M.; Forsyth, C.; Collins, C.; Huang, J. *Chem. Mater.* **2001**, *13*, 558.

(21) Bakshi, P. K.; Linden, A.; Vincent, B. R.; Roe, S. P.; Adhikasavalu, D.; Cameron, T. S.; Knop, O. *Can. J. Chem.* **1994**, *72*, 1273.

(22) Moers, O.; Wijaya, K.; Henschel, D.; Blaschette, A.; Jones, P. G. *Z. Naturforsch., B* **1999**, *54*, 1420.

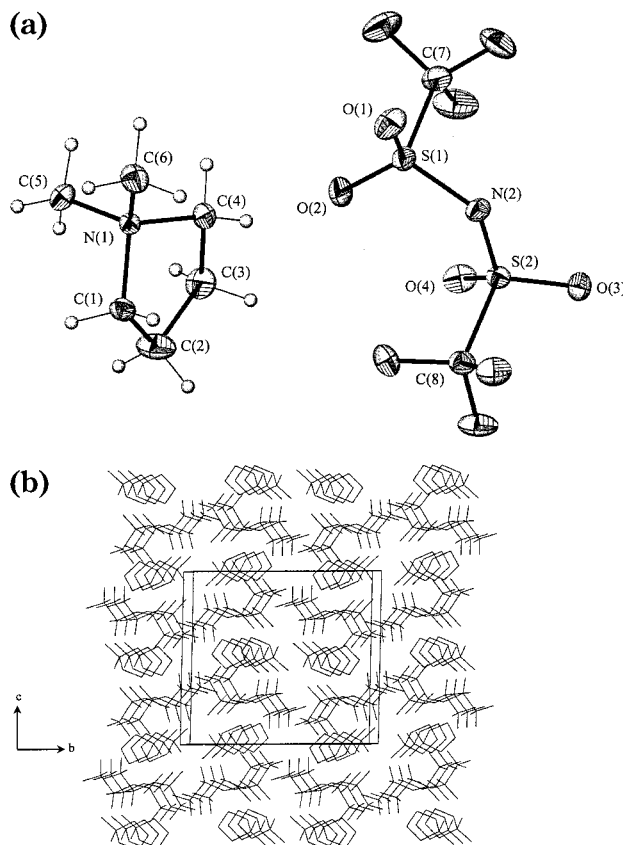


Figure 3. (a) Molecular structure of $[P11][TFSA]$ showing one ion pair. (b) The extended structure of $[P11][TFSA]$ showing the layers of cations and anions parallel to the 001 plane (hydrogen atoms have been omitted for clarity).

distances are shortened by approximately 0.07 Å presumably as a result of the lower steric demand of a CH_3 group.

An important feature of the three structures reported here is the arrangement of the ions within the crystal lattices; packing diagrams for each salt are shown in Figures 2–5. The extended structures of the $[\text{MP1}][\text{TFSA}]$, $[\text{P11}][\text{TFSA}]$, and $[\text{N111}][\text{TFSA}]$ salts (Figures 2b, 3b, and 4b) show alternating two-dimensional sheets of anions and cations parallel to the 001 plane. The MP1 layer is particularly striking (Figure 2b) with the planes of the cations parallel and approximately 45° to the 010 plane. The interplanar separation of the MP1 cations (in the *a* direction) is 8.11 Å. Successive sheets of ions in these structures have the TFSA anions situated below the interstitial spaces within the cation layer. For $[\text{N3333}][\text{TFSA}]$, chains of alternating cations and anions lie parallel to the *a*-axis, with adjacent chains displaced in the *a*-axis direction by one ion and there is no layered structure as was evident in the other three salts (Figure 5b).

In the three TFSA salts that do not have a protonated cation, the closest approaches of the cation and anion are between the sulfonyl oxygen atoms and C–H bonds on the cations (Table 4). The trimethylammonium proton of the $[\text{N111}]$ cation participates in a weak bifurcated hydrogen bond with two of the oxygen atoms (O(1) and O(3)) of the TFSA anion (Figure 5a), with N–H···O distances (Table 4) comparable to those observed in the related bis(methanesulfonyl)amide salt $[\text{Me}_2\text{NH}_2][\text{N}(\text{SO}_2\text{CH}_3)_2]$ (2.16 and 2.18 Å).²² These

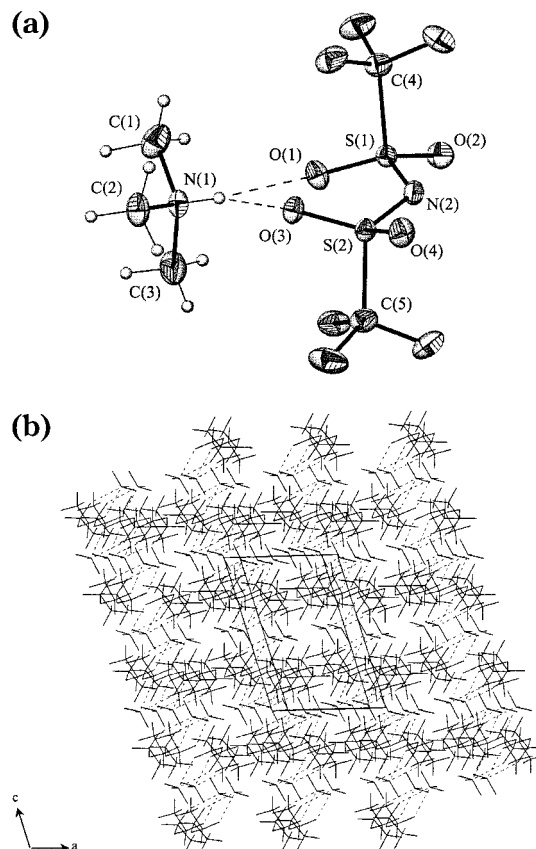


Figure 4. (a) Molecular structure of $[\text{N111}][\text{TFSA}]$ showing one ion pair. The dotted lines indicate the $\text{N–H}\cdots\text{O}$ hydrogen bonding between the N111 cation and the TFSA anion. (b) The extended structure of $[\text{N111}][\text{TFSA}]$ showing the layers of cations and anions parallel to the 001 plane with dotted lines indicating the position of $\text{N–H}\cdots\text{O}$ hydrogen bonding (hydrogen atoms have been omitted for clarity).

Table 2. Selected Bond Distances (Å) and Angles (deg) for the MP1 Cation

Cation Distances			
$\text{N(1)}-\text{C(1)}$	1.179(6)	$\text{C(1)}-\text{C(2)}$	1.546(8)
$\text{N(1)}-\text{C(4)}$	1.504(8)	$\text{C(1)}-\text{C(5)}$	1.468(8)
$\text{N(1)}-\text{C(6)}$	1.449(6)	$\text{C(2)}-\text{C(3)}$	1.508(8)
$\text{C(3)}-\text{C(4)}$	1.55(1)		
Cation Angles			
$\text{C(1)}-\text{N(1)}-\text{C(4)}$	116.2(6)	$\text{N(1)}-\text{C(1)}-\text{C(5)}$	127.6(6)
$\text{C(1)}-\text{N(1)}-\text{C(6)}$	130.9(5)	$\text{C(2)}-\text{C(1)}-\text{C(5)}$	118.8(6)
$\text{C(4)}-\text{N(1)}-\text{C(6)}$	112.8(5)	$\text{C(1)}-\text{C(2)}-\text{C(3)}$	101.4(4)
$\text{N(1)}-\text{C(1)}-\text{C(2)}$	113.5(5)	$\text{C(2)}-\text{C(3)}-\text{C(4)}$	107.4(4)

Table 3. Selected Bond Distance (Å) and Angle (deg) Ranges for the TFSA Anions

Anion Distances	
N–S	1.569(2)–1.582(2)
S–O	1.415(2)–1.436(1)
S–C	1.822(3)–1.834(2)
Anion Angles	
S–N–S	124.37(8)–124.7(1)
N–S–C	102.11(7)–104.6(1)
N–S–O	107.40(9)–117.17(8)
O–S–O	118.17(9)–119.2(1)
C–S–O	103.1(1)–105.2(2)

$\text{H}\cdots\text{O}$ separations are longer than classical hydrogen bond $\text{O–H}\cdots\text{O}$ or $\text{O–H}\cdots\text{N}$ distances (≤ 2.0 Å), which are evident in the structure of $[\text{Mg}(\text{OH}_2)_6][\text{TFSA}] \cdot (\text{H}_2\text{O})_2$ ¹² and approach the sum of the van der Waals radii (Table 4). Hence, these contacts are likely to be

Table 4. Selected Interionic Distances (Å)

	[MP1][TFSA]	[P11][TFSA]	[N111][TFSA]	[N3333][TFSA]
C—H···O (2.83) ^a	2.26	2.31(2)	2.55(2)	2.22
C···O (3.54) ^a	3.089(6)	3.199(2)	3.445(2)	3.172(6)
N—H···O (2.83)			2.22(2)	
N···O (3.14)			2.869(2)	
C—H···F (2.67) ^a	2.58	2.62	2.85	2.62
C—H···N (2.89) ^a	2.64	2.87	2.82	2.72
ion–ion separations				
N _(cat) ···N _(TFSA) (N _(cat) ···I) ^b	3.56	4.54 (4.30)	4.13	4.26 (4.65)
	5.20	5.19 (4.37)	4.60	6.12 (4.85)
	5.73	5.73 (4.40)	5.18	6.12 (4.97)
	6.83	6.28 (4.99)	6.20	6.80 (5.29)
N _(TFSA) ···N _(TFSA) (I···I) ^b	6.72	6.45 (5.46)	7.57	7.97 (7.21)
N _(cat) ···N _(cat) (N _(cat) ···N _(cat)) ^b	5.61	5.81 (6.07)	6.16	7.42 (7.23)

^a Values in parentheses are the sum of the van der Waals radii.^{23,24} ^b Values in parentheses are for the corresponding iodide salts [P11][I],¹⁹ [N3333][I].²¹

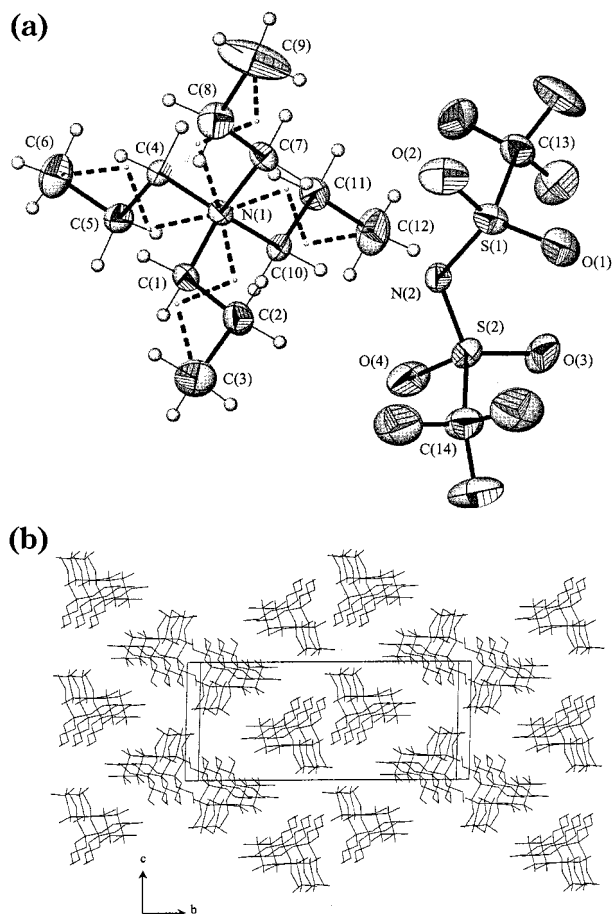


Figure 5. (a) Molecular structure of [N3333][TFSA] showing one ion pair. The dotted lines indicate the position of the second component of the disordered N3333 cation. (b) The extended structure of [N3333][TFSA] showing the chains of alternating cations and anions running parallel to the *a*-axis (hydrogen atoms have been omitted for clarity).

very weak and their influence on the melting temperature of these salts would appear to be negligible. Corresponding C—H···I (C···I) separations, ≥ 3.01 Å (3.94 Å) in [P11][I],²⁰ also approach the van der Waals limits, 3.05–3.41 Å (3.76–4.13 Å),^{23,24} but the melting temperature of the iodide salt is considerably higher

than that of the TFSA salt. Furthermore, for less polarizable anions such as BF_4^- , for which these attractive interactions should be weaker, the melting temperatures of comparable salts (e.g., [P11][BF₄], 380 °C(dec);²⁵ [N3333][BF₄], 238 °C(dec)¹⁸) are at least 100 °C higher than for the corresponding TFSA salts. Consequently, the presence of the C—H···O contacts in the TFSA salts is not the most significant influence on the physical properties of these materials.

The dominant interactions in the solid-state structures of these organic TFSA salts would appear to be the Coulombic attraction between the oppositely charged ions. The large and irregularly shaped TFSA anion significantly influences the packing of the ions within the crystal lattice as can be seen by comparison of the ion–ion separations in the TFSA salts (approximated by the N(cation)···N(anion) vectors (Table 4) with those (N(cation)···I vectors) of the corresponding iodide salts for the P11 and N3333 cations (Table 4) for which solid-state structures are known.^{20,26} It is immediately apparent that the TFSA salts have one close cation–anion separation with the remainder being significantly larger while the iodide salts have a more even range of distances, and all are shorter than the second closest cation–anion separation for the corresponding TFSA salt. This is clearly due to the spherical shape of the iodide, and indeed the molar volumes (per ion pair) for the iodide salts (P11, 0.132; N3333, 0.230 L mol⁻¹) are considerably smaller compared to the corresponding TFSA analogues (P11, 0.224; N3333, 0.333 L mol⁻¹). Thus, the ions in the TFSA salts are unable to pack as efficiently, and this combined with the diffuseness of the negative charge on the TFSA anion presumably contribute to the depression of the melting points of the TFSA salts.

A further aspect of these structures relates to the appreciable solid-state conductivities exhibited by some organic TFSA salts ($\sim 10^{-6}$ S cm⁻¹)^{6,7} compared to [Li(TFSA)]_∞ and the dramatic increase observed when these materials are doped with 1–5 mol % of [Li(TFSA)]_∞.^{4,5} The process of ion transport in the solid may involve the presence of defects in the crystal (undetectable in a single-crystal diffraction experiment) with

(23) Nyburg, S. C.; Faerman, C. H. *Acta Crystallogr., Sect. B* **1985**, *41*, 274.

(24) Pauling, L. *The Nature of the Chemical Bond*; Cornell University Press: Ithaca, 1942; p 192.

(25) Forsyth, S.; Golding, J.; MacFarlane, D. R.; Forsyth, M. *Electrochim. Acta* **2001**, *46*, 1753.

(26) Yoshida, T.; Nagata, K.; Yasuniwa, M.; Yoshimatsu, M. *Acta Crystallogr., Sect. C* **1994**, *50*, 1758.

unoccupied lattice sites allowing translational movement of ions. High conductivities are also often associated with ionic plastic phases in which it is proposed that there is considerable ion motion (rotational and translational). These types of materials have been studied by X-ray powder diffraction (see, for example, ref 27 and references therein). The highest temperature plastic phases are usually cubic and are considered to involve rapid isotropic motion of the constituent ions, thereby approximating large spherical ions, which typically pack in a CsCl type arrangement. The largest anion studied, CF_3CO_2^- , has a rotation radius of 2.68 Å²⁷ and is considerably smaller than the bulky TFSA anion with an approximate radius of 3.6 Å. Consequently, isotropic motion of the TFSA anion would be expected to be considerably more hindered than in the previously studied ionic plastic phases. However, restricted motion of the anions and/or motion of the organic cations within the anion sublattice may be possible and certainly in-plane rotation of the MP1 cation would appear to be energetically feasible given the disorder of this cation in the TFSA salt (see above). Thus, while the occurrence of isotropic motion of both ions in the TFSA salts prior to melting would appear to be unlikely, considerable anisotropic ion motion may possibly lead to plastic behavior in some of the organic TFSA salts. This conclusion is supported by entropy of fusion (ΔS_f) data. The entropy of fusion of plastic crystal phases is often $<20 \text{ J K}^{-1} \text{ mol}^{-1}$ as noted by Timmermans.²⁸ Indeed, a number of alkyl methyl pyrrolidinium hexafluorophosphate salts having plastic properties have been shown to exhibit low values of ΔS_f .²⁰ By comparison, plastic salts of the same cations with the TFSA anion exhibit ΔS_f values around $40 \text{ J K}^{-1} \text{ mol}^{-1}$ and it was hypothesized that this was a result of rotatory motion of the cation alone in the case of these salts.⁶

The doping of the organic TFSA salts with up to about 5 mol % $[\text{Li}(\text{TFSA})]_{\infty}$ results in the substitution of some of the organic cations with Li^+ in the lattice.⁴ In this range of $[\text{Li}(\text{TFSA})]_{\infty}$ concentrations, thermodynamic data indicate a region of solid solutions.⁵ As can be seen from the structure of $[\text{Li}(\text{TFSA})]_{\infty}$ itself,⁹ strong interactions occur between the oxophilic Li^+ cation and the sulfonyl oxygen atoms of the TFSA salt. Since there are

no such interactions in the organic TFSA salts to compete with, it would seem reasonable for the doped Li^+ cation to be closely associated with one or possibly more of the TFSA anions. The disparity in size and shape of the Li^+ and the organic cations would therefore create a significant disruption of the crystal lattice at that point that may allow an increase in ion mobility. In higher temperature plastic crystal phases, where rotatory ion motion can lead to extensive vacancy or defect formation, the conduction mechanism is likely to be dominated by diffusion of these vacancies or defects. We have previously seen evidence for some Li^+ ion and pyrrolidinium cation translational diffusion, although only a fraction of the organic cations are diffusing in comparison to all of the lithium cations.²⁹

Summary

The single-crystal structure data for four organic TFSA salts show isolated ion pairs with little significant interionic contacts throughout the crystal lattices, even in the presence of a suitable hydrogen bond donor. The diffusivity of the negative charge on the TFSA anion and the inefficient packing of these irregularly shaped ions appear to be the major contributors to the observed physical properties (low melting, solid-state ionic conductivity, and ionic plastic phases) which are related to ease of ion motion in these and related materials. Several of the TFSA salts exhibited two-dimensional layered structures that may further facilitate ionic conductivity in the solid state. The current data provide a basis for detailed examination of possible ion transport mechanisms in the Li^+ -doped organic TFSA salts, and this will be the subject of future work.

Acknowledgment. This research was supported by the Australian Research Council and is gratefully acknowledged.

Supporting Information Available: Tables of crystal data, structure solution and refinement, atomic coordinates, bond distances and angles, and anisotropic thermal parameters for $[\text{MP1}][\text{TFSA}]$, $[\text{P11}][\text{TFSA}]$, $[\text{N111}][\text{TFSA}]$, and $[\text{N3333}][\text{TFSA}]$ (PDF). This material is available free of charge via the Internet at <http://pubs.acs.org>.

CM0107777

(27) Kuchitsu, K.; Ono, H.; Ishimaru, S.; Ikeda, R.; Ishida, H. *Phys. Chem. Chem. Phys.* **2000**, 2, 3883.

(28) Timmermans, J. *J. Phys. Chem. Solids* **1961**, 18, 1.

(29) Every, H. Ph.D. Thesis, Monash University, 2001.